Comparisons of Finite Difference Beam Propagation Methods for Modeling Second-Order Nonlinear Effects

Hsu-Feng Chou, Ching-Fuh Lin, *Member, IEEE, Member, OSA,* and Shing Mou

***Abstract*—Three numerical methods, iterative finite difference (FD), split-step, and iterative split-step beam propagation methods (BPM's), for modeling second-order nonlinear effects are evaluated. All three methods are able to handle the depletion of the pump wave. The evaluation shows that both iterative methods are more accurate than the split-step method. In addition, the iterative split-step method, even with its iterative nature, is more efficient than the split-step one. Between the two iterative methods, further comparisons indicate that, for a small stepsize, both have comparable accuracy. As the stepsize increases, the iterative split-step method is not as accurate as the iterative finite-difference one. However, the former method has a higher efficiency, suggesting that it is a better choice when the stepsize has to be small because of, for example, the quasiphase-matched geometrical configuration.**

***Index Terms*— Finite difference beam propagation method (FD/BPM), quasi-phase matching, second harmonic generation, second-order nonlinear effects, split-step beam propagation method.**

I. Introduction

DUE to the versatile and efficient frequency conversion ability, second-order nonlinear effects, especially those implemented with the quasi-phase matching (QPM) technique [1], [2], have potential applications in many areas. For example, the QPM second harmonic generation (SHG) [3] can provide laser sources in the visible region [4]. Other QPM second-order nonlinear effects like sum frequency generation (SFG) and difference frequency generation (DFG) are useful in frequency tripling and quadrupling [5], mid-infrared (IR) generation [6], and wavelength division multiplexing (WDM) networks [7]. Large nonlinear phase shifts induced by QPM second-order nonlinear effects [8] have also been proposed to realize all-optical switching [9] and short-pulse compression [10].

QPM devices have been successfully fabricated on ferroelectric materials such as $LiNbO_3$, $LiTaO_3$, and KTP [11]–[13] as well as semiconductors like AlGaAs [14], [15]. To understand the function of these devices, theoretical modeling for the QPM nonlinear effects is important. Although analytical analyzes had been done to provide a quick insight into QPM nonlinear effects, many approximations are required for those analyzes [16]–[19]. When large or irregular geometrical variations exist and the depletion of the pump wave is not negligible, precise analytical modeling of these second-order nonlinear devices becomes quite difficult. For a general and accurate analysis, numerical methods are required. The beam propagation method (BPM) [20] is a powerful and flexible approach to design and simulate linear optical devices. It had also been extended to simulate second-order nonlinear effects based on schemes such as fast Fourier transform (FFT) [21], finite element (FE) [22]–[24], and finite difference (FD) methods [25]–[30].

In the past, the numerical methods for nonlinear effects, mostly for SHG, still assume that the fundamental wave is independent of the propagation distance. This assumption greatly simplifies the treatment of the nonlinear terms. However, in devices where the conversion efficiency is high or where there is a geometrical variation of the waveguide structure, this assumption is not valid. Therefore, methods being able to deal with the depletion of the fundamental wave are necessary. In this paper, we evaluate three such methods. The scope will be restricted exclusively to the finite difference category because it is mostly preferred for better efficiency and accuracy and is more easily implemented than FFT or FE methods [20], [31]. The comparisons will be done only in one- and two-dimensional (1-D) and (2-D) cases, which is sufficient for lucid manifestation of these BPM algorithms. Without loss of generality, the formulations below are given for the SHG case. The extension to the general three-frequency situation is straightforward.

II. Formulation

Employing paraxial approximation, the wave equation in the presence of nonlinear polarization is reduced to the following form:

$$2jk_{os}\overline{n}_s\frac{\partial E_s}{\partial z}=\frac{\partial^2 E_s}{\partial x^2}+k_{os}^2(n_s^2-\overline{n}_s^2)E_s+k_{os}^2\chi^{(2)}e^{-j\cdot\Delta k\cdot z}E_fE_f \tag{1a}$$

$$2jk_{of}\overline{n}_f\frac{\partial E_f}{\partial z}=\frac{\partial^2 E_f}{\partial x^2}+k_{of}^2(n_f^2-\overline{n}_f^2)E_f+2k_{of}^2\chi^{(2)}e^{j\cdot\Delta k\cdot z}E_sE_f^* \tag{1b}$$

Manuscript received August 20, 1998; revised April 5, 1999. This work was supported in part by the National Science Council, Taipei, Taiwan, R.O.C., under Contract NSC87-2215-E-002-012.

The authors are with the Institute of Electro-Optical Engineering and the Department of Electrical Engineering, National Taiwan University Taipei, Taiwan, R.O.C.

Publisher Item Identifier S 0733-8724(99)06347-1.

where $\overline{n}$, k_o, $\chi^{(2)}$and E are the effective index of the guided mode, the wave vector in free space, the nonlinear susceptibility, and the slowly varying envelope of the field, respectively. Subscripts s and f represent the second harmonic and the fundamental waves, respectively, and $\Delta k \equiv 2\overline{n}_f k_{of} - \overline{n}_s k_{os}$. Note that the definition of $\chi^{(2)}$ here is the same as what is usual and differs from our previous paper [30] by a factor of one-half. Propagation along the z direction is assumed. For concise expressions, the following finite difference operators are defined:

$$L_x E_i^{m,\ell} = \frac{1}{\Delta x^2}\left(E_i^{m-1,\ell} - 2E_i^{m,\ell} + E_i^{m+1,\ell}\right) \quad (2a)$$

$$L_{oi}^{m,\ell} = k_{oi}^2\left(n_i^{m,\ell^2} - \overline{n}_i^2\right), \qquad i = s, f \quad (2b)$$

$$F_s^{m,\ell} = k_{os}^2 \chi^{(2)^{m,\ell}} e^{-j\cdot\Delta k\cdot\ell\cdot\Delta z} \quad (2c)$$

$$F_f^{m,\ell} = 2k_{of}^2 \chi^{(2)^{m,\ell}} e^{j\cdot\Delta k\cdot\ell\cdot\Delta z}. \quad (2d)$$

Note that $E_{m,\ell}$ represents the electric field at the point $(x, z) = (m\cdot\Delta x, \ell\cdot\Delta z)$.

A. IFD-BPM

In the IFD-BPM [30], the difference equations involve undetermined nonlinear source terms in the next step, and iterative schemes [32]–[34] are required to solve this problem. The fixed-point iteration [34] is chosen for the IFD-BPM. It has the advantage of great simplicity and requires the minimal modification from the linear BPM, compared with other iterative methods. The IFD-BPM is briefly described in the following. First, one set of solution, $E^{(0)}$, the initial guess of the electric fields in the iterative algorithm, is obtained by some simpler methods such as the EFD-BPM [26] or the rectangular approximation (RA) scheme [30]. This algorithm can be expressed as

$$\begin{aligned}\frac{2jk_{os}\overline{n}_s}{\Delta z}&\left(E_s^{m,\ell+1^{(t)}} - E_s^{m,\ell}\right)\\ &= \tfrac{1}{2}\Big[\left(L_x + L_{os}^{m,\ell+1/2}\right)\left(E_s^{m,\ell} + E_s^{m,\ell+1^{(t)}}\right)\\ &\quad + \Big(F_s^{m,\ell}E_f^{m,\ell}E_f^{m,\ell}\\ &\quad + F_s^{m,\ell+1}E_f^{m,\ell+1^{(t-1)}}E_f^{m,\ell+1^{(t-1)}}\Big)\Big]\end{aligned} \quad (3a)$$

$$\begin{aligned}\frac{2jk_{of}\overline{n}_f}{\Delta z}&\left(E_f^{m,\ell+1^{(t)}} - E_f^{m,\ell}\right)\\ &= \tfrac{1}{2}\Big[\left(L_x + L_{of}^{m,\ell+1/2}\right)\left(E_f^{m,\ell} + E_f^{m,\ell+1^{(t)}}\right)\\ &\quad + \Big(F_f^{m,\ell}E_s^{m,\ell}E_f^{m,\ell^*}\\ &\quad + F_f^{m,\ell+1}E_s^{m,\ell+1^{(t-1)}}E_f^{m,\ell+1^{(t-1)^*}}\Big)\Big]\end{aligned} \quad (3b)$$

where t is the iteration count, starting from one, and $E^{(t)}$ is the tth iteration field. In this study, RA scheme is used to obtain the initial guess.

B. SS-BPM

Split-step methods [35], sometimes called operator splitting methods in some literature [32], are commonly used for time-dependent partial differential equations. They are often applied to reduce problems in multidimensional space to a sequence of problems in one dimension and can significantly reduce the work required for implicit methods. In [28] and [29], the split-step method is applied to (1) so that each propagation step is split into two sequential steps: one deals with only linear propagation of the waves while the other takes care of the nonlinear coupling between different frequencies. In our notation, the method presented in [29] can be reexpressed as follows.

Step 1) Linear:

$$\begin{aligned}\frac{2jk_{os}\overline{n}_s}{\Delta z}&\left(E_s^{m,\ell+1^{(I)}} - E_s^{m,\ell}\right)\\ &= \tfrac{1}{2}\left(L_x + L_{os}^{m,\ell+1/2}\right)\left(E_s^{m,\ell} + E_s^{m,\ell+1^{(I)}}\right)\end{aligned} \quad (4a)$$

$$\begin{aligned}\frac{2jk_{of}\overline{n}_f}{\Delta z}&\left(E_f^{m,\ell+1^{(I)}} - E_f^{m,\ell}\right)\\ &= \tfrac{1}{2}\left(L_x + L_{of}^{m,\ell+1/2}\right)\left(E_f^{m,\ell} + E_f^{m,\ell+1^{(I)}}\right).\end{aligned} \quad (4b)$$

Step 2) Nonlinear:

$$\begin{aligned}E_s^{m,\ell+1} &= \cos(\Delta z\cdot\Phi)\cdot E_s^{m,\ell+1^{(I)}}\\ &\quad - j\cdot\Omega\cdot\sin(\Delta z\cdot\Phi)\cdot E_f^{m,\ell+1^{(I)}}\end{aligned} \quad (5a)$$

$$\begin{aligned}E_f^{m,\ell+1} &= \cos(\Delta z\cdot\Phi)\cdot E_f^{m,\ell+1^{(I)}}\\ &\quad - j\cdot\Omega\cdot\sin(\Delta z\cdot\Phi)\cdot E_s^{m,\ell+1^{(I)}}\end{aligned} \quad (5b)$$

where

$$\Phi = \frac{k_{of}\cdot\chi^{(2)}}{\sqrt{\overline{n}_f\overline{n}_s}}\left|E_f^{m,\ell+1^{(I)}}\right|$$

$$\Omega = \sqrt{\frac{\overline{n}_s}{\overline{n}_f}}e^{-j\cdot\delta k\cdot z}E_f^{m,\ell+1^{(I)}} \Big/ \left|E_f^{m,\ell+1^{(I)}}\right|.$$

$\overline{n}_f$ and $\overline{n}_s$ are the effective refractive indexes of the fundamental and the SH waves, respectively. The superscript (I) denotes the corresponding intermediate field. Note that when dealing with the nonlinear terms, it is assumed in the SS-BPM that the coupling between frequencies is constant within each propagation step. In [29], improvements on the accuracy of the nonlinear step are also mentioned, which involve repeated execution of the procedures in Step 2). However, as will be clearly shown later, these are not economical approaches since the second step of the SS-BPM takes much longer computation time than that of the ISS-BPM.

C. ISS-BPM

In this paper, we propose a hybrid method, the iterative split-step BPM (ISS-BPM), which combines the iterative and the split-step methods. In the next section, it will be shown that the ISS-BPM is more efficient and accurate than the SS-BPM. There are also two steps in the ISS-BPM. The first step considers only the linear propagation and is identical to that of the SS-BPM. The second step employs the fixed-point iteration as in the IFD-BPM to handle the nonlinear coupling terms. The ISS-BPM is expressed as follows.

Step 2) Nonlinear:

$$\frac{2jk_{os}\overline{n}_s}{\Delta z}\left(E_s^{m,\ell+1^{(t)}} - E_s^{m,\ell+1^{(I)}}\right) = \tfrac{1}{2}\left(F_s^{m,\ell}E_f^{m,\ell+1^{(I)}}E_f^{m,\ell+1^{(I)}} + F_s^{m,\ell+1}E_f^{m,\ell+1^{(t-1)}}E_f^{m,\ell+1^{(t-1)}}\right) \tag{6a}$$

$$\frac{2jk_{of}\overline{n}_f}{\Delta z}\left(E_f^{m,\ell+1^{(t)}} - E_f^{m,\ell+1^{(I)}}\right) = \tfrac{1}{2}\left(F_f^{m,\ell}E_s^{m,\ell+1^{(I)}}E_f^{m,\ell+1^{(I)^*}} + F_f^{m,\ell+1}E_s^{m,\ell+1^{(t-1)}}E_f^{m,\ell+1^{(t-1)^*}}\right). \tag{6b}$$

The iteration is performed in Step 2), which is similar to the IFD-BPM but without linear terms. Note that in this work, the initial guess $E^{(o)}$ is obtained by the RA scheme [30].

III. Comparison

For comparison purposes, a 1-D plane-wave, fully birefringent-phase-matched SHG case is simulated first. In this case, analytical solutions exist and can be used to examine the numerical results. With the initial power of the SH equal to zero, the intensities of the fundamental and the SH waves are given by

$$I_s = I_o^f \tanh^2(\Gamma z) \tag{7a}$$

$$I_f = I_o^f \mathrm{sech}^2(\Gamma z) \tag{7b}$$

where $\Gamma = k_o^f \chi^{(2)}|E_o^f|/$ and E_o^f are the initial intensity, the free-space wavevector and the field amplitude of the fundamental wave. n_f and n_s are the refractive indexes of the fundamental and the SH waves. In the simulation, they are both set to 2.2. The wavelengths of the two waves are 0.808 μm and 0.404 μm. The nonlinear susceptibility, $\chi^{(2)}$, is 85 pm/V. The initial power levels of the fundamental and the SH waves are 4 and 0 W, respectively.

The normalized intensities calculated analytically and by various numerical methods are plotted in Fig. 1(a), in which no difference can be observed. For detailed comparison, the absolute differences between the analytical and the numerical solutions are plotted in Fig. 1(b). Note that the RA scheme [30] provides initial guesses for the iterative methods. In the 1-D situation, there are no diffraction terms, so the ISS-BPM is exactly identical to the IFD-BPM. This figure shows that the iterative method converges substantially right after the first iteration. However, for the SS-BPM, even with a stepsize that is five times smaller, the result is still less accurate than those of the ISS-BPM. Moreover, the SS-BPM takes longer computation time than the ISS-BPM with one iteration. The computation times required by different schemes with the same stepsize are in the following ratio:

$$\text{RA} : \text{1 IT} : \text{2 IT} : \text{3 IT} : \text{SS-BPM} = 1 : 2 : 3.3 : 4.5 : 3.6$$

where 1 IT represents one iteration and similarly for 2 IT and 3 IT. It is possible to improve the accuracy of the SS-BPM to the extent similar to 1 IT [29], but the computation time will be more than doubled. As a result, the SS-BPM will be much slower than the ISS-BPM with one iteration for the same accuracy. The bottleneck of the SS-BPM is in the evaluation of trigonometric functions.

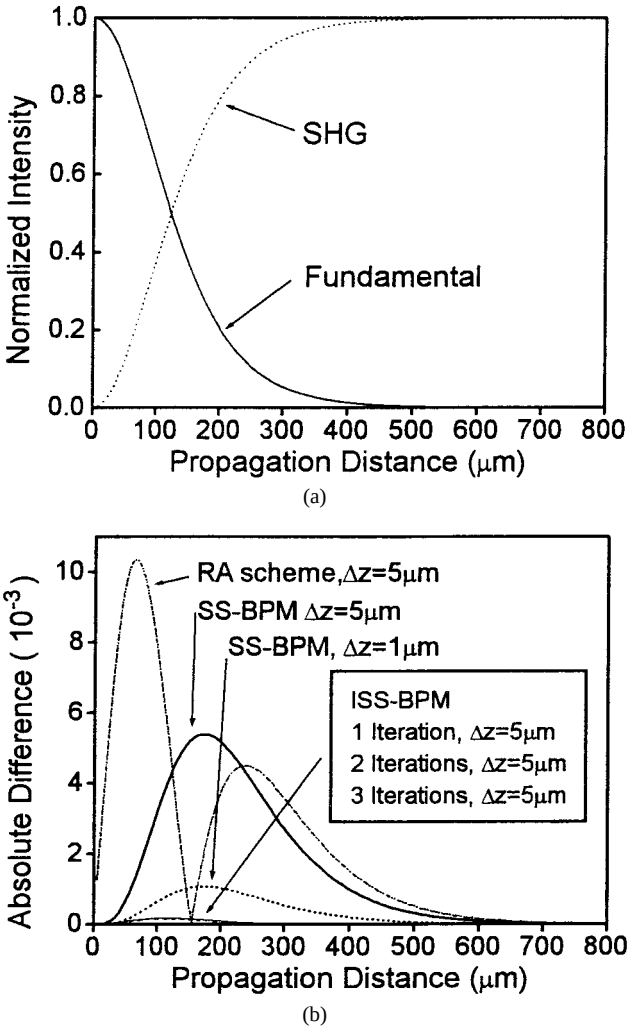

Fig. 1. (a) The normalized intensities of the fundamental and the SH waves calculated analytically and by different numerical schemes. (b) Absolute difference of normalized fundamental intensities between the analytical solution and the result obtained by different numerical methods.

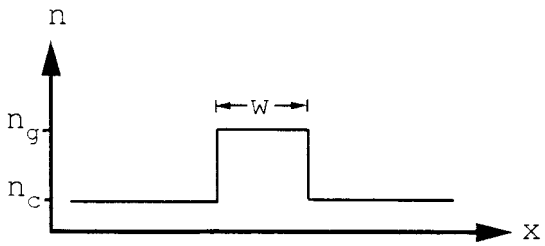

Fig. 2. The index profile along the x-axis. w, n_g, and n_c are the width of the waveguide and the refractive indexes of the guiding and the cladding layers, respectively.

Next, a 2-D birefringent phase-matched SHG case is used for comparison. Due to the discrete nature of the FD methods, different stepsizes could cause different period irregularities of the $\chi^{(2)}$ modulation and so lead to extra calculation error. Then the stepsize in the numerical calculation for QPM condition has more or less influences on the convergence rate. Therefore,

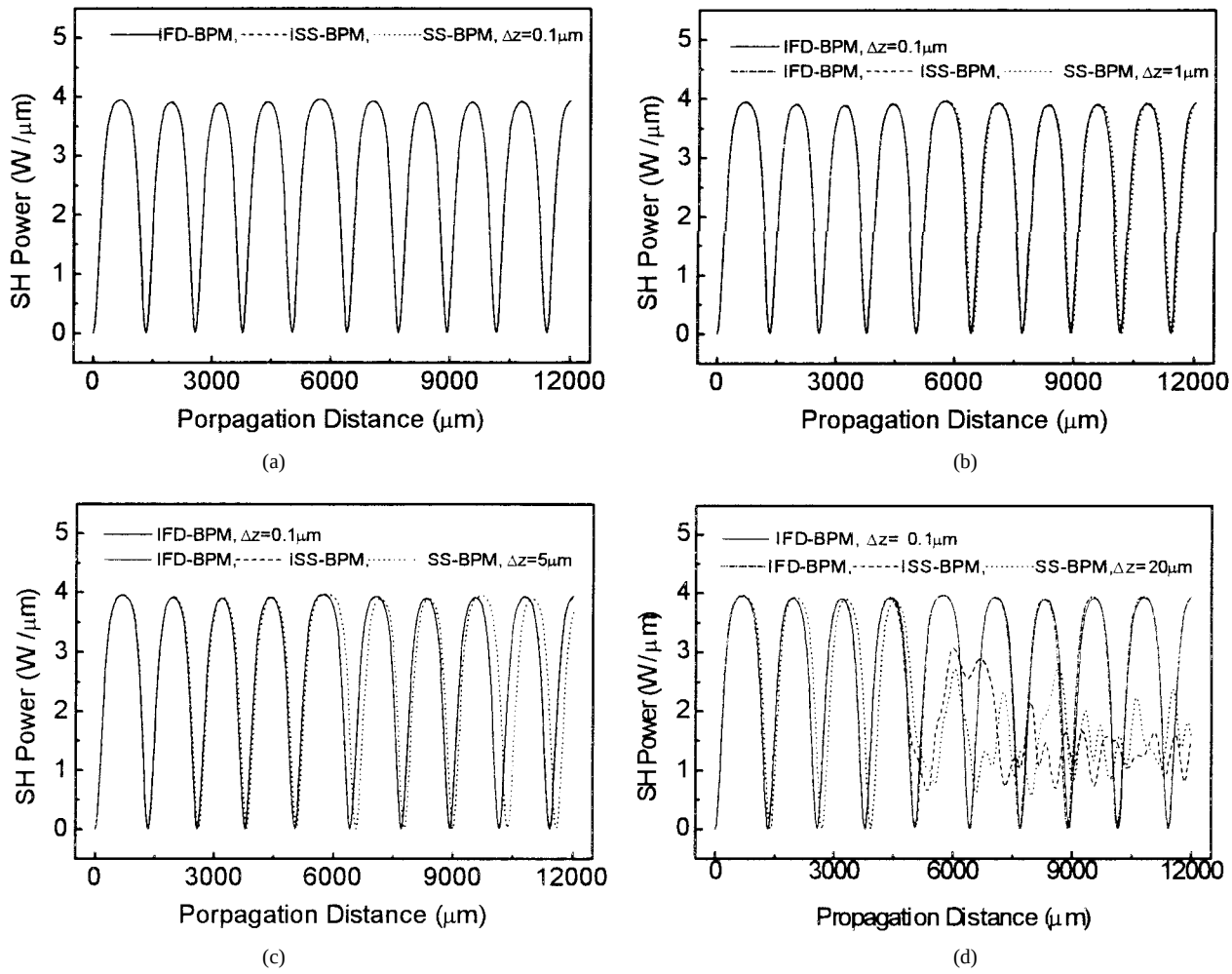

Fig. 3. The simulated SH power variation along the propagation direction for (a) $\Delta z = 0.1$ μm, (b) $\Delta z = 1$ μm, (c) $\Delta z = 5$ μm, and (d) $\Delta z = 20$ μm.

a birefringent phase-matched case is use here for studying the convergence rate. The configuration is a straight waveguide as shown in Fig. 2, where w, n_g, and n_c are the width of the waveguide and the refractive indexes of the guiding and the cladding layers. The wavelengths and the refractive indexes of the fundamental and the SH waves are 0.808 μm, 0.404 μm, 2.32723, and 2.32679, respectively. For evaluation purposes, a typical value of the index difference of the waveguide, $\Delta n = n_g - n_c = 0.002$, is used for both frequencies. The width of the waveguide w is 4 μm and $\chi^{(2)}$ is 46.5 pm/V. The initial power levels of the fundamental and the SH waves are 4 and 0 W/μm. The computation window is 40 μm wide with $\Delta x = 0.2$ μm for all methods. The SH power at $z = \ell \cdot \Delta z$ is defined as

$$\frac{\Delta x}{\eta_o}\overline{n}_s \sum_m \left|E_s^{m,\ell}\right|^2 \tag{8}$$

where η_o is the free-space impedance, and the summation, m, runs over the discretization points along the x-direction. The unit is in W/unit length because of the 2-D configuration. The power diagrams of the SH wave for the four stepsizes, 0.1, 1, 5, and 20 μm, are shown in Fig. 3(a)–(d), respectively. Only one iteration is executed for the iterative methods. Fig. 3(a) shows that, with $\Delta z = 0.1$ μm, the results obtained by the three schemes are indistinguishable, which means that they all converge and agree with one another. Without loss of generality, the power diagram calculated by the IFD-BPM with $\Delta z = 0.1$ μm is used as a reference in other figures. As can be seen from Fig. 3(b) and (c), the power diagrams calculated by the SS-BPM deviate progressively from the reference as the stepsize increases while the results obtained by the other two schemes remain almost the same. To be more specific, the SS-BPM predicts a slower conversion of the SHG. This lag of interaction may be attributed to the approximation of constant coupling.

As the stepsize increases further, as shown in Fig. 3(d), the results calculated by both ISS-BPM and SS-BPM become inaccurate. It is interesting to note that the deviation is not gradual. Instead, it deviates from the reference curve outrageously after some critical distance. Similar behavior had been observed for the EFD-BPM [30]. This precipitous behavior probably results from the exponentially accumulated numerical error. On the other hand, the result calculated by the IFD-BPM, even with $\Delta z = 20$ μm, still agrees with the reference very well. For a closer investigation, the convergence of field is shown in Fig. 4(a) and (b) for $\Delta z = 0.1$ and 15 μm, respectively. Fig. 4(a) shows that the fields calculated by the three schemes with $\Delta z = 0.1$ μm after 12 000

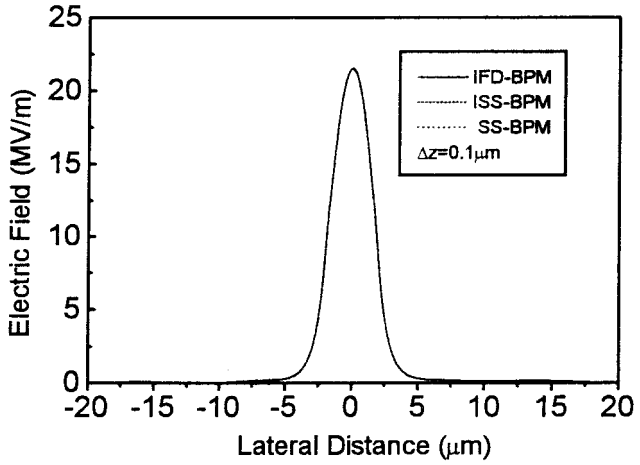

(a)

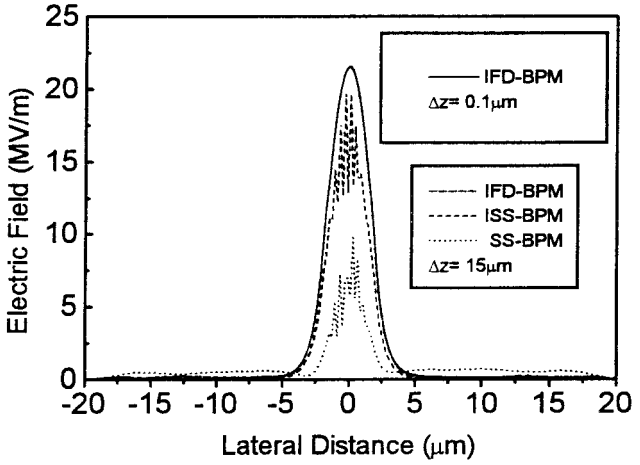

(b)

Fig. 4. Time averaged SH field profiles after 12 000 μm of propagation calculated by different methods with different stepsizes: (a) $\Delta z = 0.1$ μm and (b) $\Delta z = 15$ μm.

μm of propagation distance remain the same. However, with $\Delta z = 15$ μm, only the field calculated by IFD-BPM closely resembles the one with $\Delta z = 0.1$ μm, as shown in Fig. 4(b).

The above comparisons show that ISS-BPM has better accuracy and efficiency than the published SS-BPM. Between the two iterative methods, ISS-BPM has a worse convergence rate than the IFD-BPM for large stepsizes, but the former one has a better efficiency. Depending on the way the initial guess used in IFD-BPM, usually about 33–50% of computation time can be saved if ISS-BPM is used. For numerical calculation in QPM, the stepsize cannot be large in order to minimize the possible error due to the period irregularities caused by the discrete of FD method. Then, ISS-BPM could be a better choice in the consideration of efficiency.

IV. Conclusion

Three numerical methods, IFD-BPM, SS-BPM and ISS-BPM, for modeling second-order nonlinear effects are evaluated. All three methods are able to handle the depletion of the pump wave. From the above evaluations, the newly proposed hybrid method, ISS-BPM, was shown to be more efficient and accurate than the SS-BPM. When compared to our previously published IFD-BPM, ISS-BPM has a lower stepsize convergence rate. However, if the stepsize is small enough, ISS-BPM is almost as accurate as IFD-BPM and it could save about 33–50% computation time. Therefore, when the stepsize has to be small because of the QPM geometrical configuration, ISS-BPM should be a better choice for efficiency reason.

Acknowledgment

The authors would like to thank Prof. H.-C. Chang, M.-C. Yang, and Y.-L. Hsueh for their helpful discussions.

References

[1] S. Somekh and A. Yariv, "Phase matching by periodic modulation of the nonlinear optical properties," *Opt. Commun.*, vol. 6, pp. 301–304, 1972.
[2] L. E. Myers, R. C. Eckardt, M. M. Fejer, and R. L. Byer, "Quasiphase-matched optical parametric oscillations in bulk periodically poled $LiNbO_3$," *J. Opt. Soc. Amer. B*, vol. 12, pp. 2102–2116, 1995.
[3] M. M. Fejer, G. A. Magel, D. H. Jundt, and R. L. Byer, "Quasiphase-matched second harmonic generation: Tuning and tolerances," *IEEE J. Quantum Electron.*, vol. 28, pp. 2631–2654, 1992.
[4] J. Webjorn, S. Siala, D. K. Nam, R. G. Waarts, and R. J. Lang, "Visible laser sources based on frequency doubling in nonlinear waveguides," *IEEE J. Quantum Electron.*, vol. 33, pp. 1673–1685, 1997.
[5] O. Pfister, J. S. Wells, L. Hollberg, L. Zink, D. A. Van Baak, M. D. Levenson, and W. R. Bosenberg, "Continuous-wave frequency tripling and quadrupling by simultaneous three-wave mixing in periodically poled crystal: Application to a two-step 1.19–10.71-μm frequency bridge," *Opt. Lett.*, vol. 22, pp. 1211–1213, 1997.
[6] L. Goldberg and W. K. Burns, "Wide acceptance bandwidth difference frequency generation in quasiphase-matched $LiNbO_3$," *Appl. Phys. Lett.*, vol. 67, pp. 2910–2912, 1995.
[7] C. Q. Xu, H. Okayama, and T. Kamijoh, "Broadband multichannel wavelength conversions for optical communication systems using quasiphase matched difference frequency generation," *Japan J. Appl. Phys.*, vol. 34, pp. L 1543–L 1545, 1995.
[8] M. L. Sundheimer, Ch. Bosshard, E. W. Van Stryland, and G. I. Stegeman, "Large nonlinear phase modulation in quasiphase-matched KTP waveguides as a result of cascaded second-order processes," *Opt. Lett.*, vol. 18, pp. 1397–1399, 1993.
[9] C. N. Ironside, J. S. Aitchison, and J. M. Arnold, "An all-optical switch employing the cascaded second-order nonlinear effect," *IEEE J. Quantum Electron.*, vol. 29, pp. 2650–2654, 1993.
[10] M. A. Arbore, O. Marco, and M. M. Fejer, "Pulse compression during second-harmonic generation in a periodic quasiphase-matching gratings," *Opt. Lett.*, vol. 22, pp. 865–867, 1997.
[11] C. Baron, H. Cheng, and M. C. Gupta, "Domain inversion in $LiTaO_3$ and $LiNbO_3$ by electric field application on chemically patterned crystals," *Appl. Phys. Lett.*, vol. 68, pp. 481–483, 1996.
[12] M. L. Bortz and M. M. Fejer, "Annealed proton exchanged $LiNbO_3$ waveguides," *Opt. Lett.*, vol. 6, pp. 1844–1846, 1991.
[13] D. Eger, M. Oron, M. Katz, and A. Zussman, "Highly efficient blue light generation in $KTiOPO_4$ waveguides," *Appl. Phys. Lett.*, vol. 64, pp. 3208–3209, 1994.
[14] S. J. B. Yoo, C. Caneau, R. Bhat, M. A. Koza, A. Rajhel, and N. Antoniades, "Wavelength conversion by difference frequency generation in AlGaAs waveguides with periodic domain inversion achieved by wafer bonding," *Appl. Phys. Lett.*, vol. 68, pp. 2609–2611, 1996.
[15] C. Q. Xu, K. Takemasa, K. Nakamura, H. Wada, T. Takamori, H. Okayama, and T. Kamijoh, "Confirmation of AlGaAs crystal domain inversion using asymmetric wet etching and optical second-harmonic generation methods," *Japan J. Appl. Phys.*, vol. 35, pp. L 1419–L 1421, 1996.
[16] J. D. McMullen, "Optical parametric interactions in isotropic materials using a phase-corrected stack of nonlinear dielectric plates," *J. Appl. Phys.*, vol. 46, pp. 3076–3081, 1975.
[17] C. Q. Xu, H. Okayama, and M. Kawahara, "Optical frequency conversions in nonlinear medium with periodically modulated linear and nonlinear optical parameters," *IEEE J. Quantum Electron.*, vol. 31, pp. 981–987, 1995.

[18] V. Mahalakshmi, M. R. Shenoy, and K. Thyagarajan, "Evolution of the intensity profile of Cerenkov second-harmonic radiation with propagation distance in planar waveguides," *IEEE J. Quantum Electron.*, vol. 32, pp. 137–144, 1996.
[19] T. Sugihara, H. Haga, and S. Yamamoto, "Electrically tunable guided-wave optical frequency converter using dye-doped polymers," *IEEE J. Lightwave Technol.*, vol. 16, pp. 239–245, 1998.
[20] H. J. W. M. Hoekstra, "On beam propagation methods for modeling in integrated optics," *Opt. Quantum Electron.*, vol. 29, pp. 157–171, 1997.
[21] B. Hermansson, D. Yevick, and L. Thylen, "A propagating beam method analysis of nonlinear effects in optical waveguides," *Opt. Quantum Electron.*, vol. 16, pp. 525–534, 1984.
[22] K. Hayata and M. Koshiba, "Numerical study of guided-wave sum-frequency generation through second-order nonlinear parametric processes," *J. Opt. Soc. Amer. B*, vol. 8, pp. 449–458, 1991.
[23] K. Hayata and M. Koshiba, "Three-dimensional simulation of guided-wave second-harmonic generation in the form of coherent Cerenkov radiation," *Opt. Lett.*, vol. 16, pp. 1563–1565, 1991.
[24] F. A. Katsriku, B. M. A. Rahman, and K. T. V. Grattan, "Numerical modeling of second harmonic generation in optical waveguides using the finite element method," *IEEE J. Quantum Electron.*, vol. 33, pp. 1727–1733, 1997.
[25] P. S. Weitzman and U. Osterberg, "A modified beam propagation method to model second harmonic generation in optical fibers," *IEEE J. Quantum Electron.*, vol. 29, pp. 1437–1443, 1993.
[26] H. M. Masoudi and J. M. Arnold, "Modeling second-order nonlinear effects in optical waveguides using a parallel-processing beam propagation method," *IEEE J. Quantum Electron.*, vol. 31, pp. 2107–2113, 1995.
[27] H. M. Masoudi and J. M. Arnold, "Parallel beam propagation method for the analysis of second harmonic generation," *IEEE Photon. Technol. Lett.*, vol. 7, pp. 400–402, 1995.
[28] G. J. M. Krijnen, W. Torruellas, G. I. Stegeman, H. J. W. M. Hoekstra, and P. V. Lambeck, "Optimization of second harmonic generation and nonlinear phase-shifts in the Cerenkov regime," *IEEE J. Quantum Electron.*, vol. 32, pp. 729–738, 1996.
[29] H. J. W. M. Hoekstra, O. Noordman, G. J. M. Krijnen, R. K. Varshney, and E. Henselmans, "Beam-propagation method for second-harmonic generation in waveguides with birefringent materials," *J. Opt. Soc. Amer. B*, vol. 14, pp. 1823–1830, 1997.
[30] H.-F. Chou, C.-F. Lin, and G.-C. Wang, "An iterative finite difference beam propagation method for modeling second-order nonlinear effects in optical waveguides," *J. Lightwave Technol.*, vol. 16, pp. 1686–1693, 1998.
[31] Y. Chung and N. Dagli, "An assessment of finite difference beam propagation method," *IEEE J. Quantum Electron.*, vol. 26, pp. 1335–1339, 1990.
[32] W. Press, B. Flannery, S. Teukolsky, and W. Vetterling, *Numerical Recipes: The Art of Scientific Computing.* Cambridge, U.K.: Cambridge Univ. Press, 1990.
[33] J. W. Thomas, *Numerical Partial Differential Equations: Finite Difference Methods.* New York: Springer-Verlag, 1995.
[34] S. Nakamura, *Applied Numerical Methods with Software.* Englewood Cliffs, NJ: Prentice Hall, 1991.
[35] B. Gustafsson, H. Kreiss, and J. Oliger, *Time Dependent Problems and Difference Methods.* New York: Wiley, 1995.

Hsu-Feng Chou was born in Taipei, Taiwan, R.O.C., in 1974. He received the B.S. degree in physics in 1996 and the M.S. degree in electrooptical engineering in 1998 from the National Taiwan University, Taipei.

His research interest is mainly on the study of optical nonlinear effects.

Ching-Fuh Lin (M'97) was born in I-Lan, Taiwan, R.O.C., in 1961. He received the B.S. degree from the National Taiwan University, Taipei, R.O.C., and the M.S. and Ph.D. degrees from Cornell University, Ithaca, NY, in 1989 and 1993, respectively, all in electrical engineering.

In 1993, he joined the faculty of the National Taiwan University and is now a Professor in the Department of Electrical Engineering and the Institute of Electro-Optical Engineering. His current research interests include mode-locking of semiconductor lasers, ultrafast phenomena and carrier dynamics in semiconductor lasers/amplifiers, high-power semiconductor lasers/amplifiers and their applications, and semiconductor-laser-pumping technology.

Dr. Lin is a member of the IEEE Lasers and Electro-Optics Society, the American Vacuum Society, and the Optical Society of America (OSA).

Shing Mou was born in Oregon in 1976 and then moved to Taiwan, R.O.C., in 1978. He received the B.S. degree in electrical engineering from the National Taiwan University, Taipei, R.O.C., in 1998. He is now working towards the M.S. degree in the Institute of Electro-Optical Engineering at the National Taiwan University.